

S1. Inventory of the catalog of gas flaring in Russia

In this section, the composition of the gas flaring catalog spreadsheet (digital part of Supplementary Materials), sources of the information and procedures applied for data treatment are specified.

S1.1 Catalog layout

The gas flaring catalog is presented in the first list of the document (“Gas Flares in Russia_2012-2020”). The second list presents the list of oil and gas joint ventures applied in the catalog (see Section S1.5).

From the original VIIRS Nightfire algorithm annual datasets (available online at https://eogdata.mines.edu/download_global_flare.html), gas flare ID (‘ID_old’ and “ID20xx”), geographical coordinates (‘Lat’, ‘Lon’), temperature (‘T_{min}’, ‘T_{max}’, ‘T_{mean}’), detection frequency (‘Pct’), and estimated flaring volumes (‘MCM20xx’) were obtained. Regional data (federal district and federal subject subdivision of Russian Federation as of 2021), field or object (downstream plant, midstream infrastructure object) name and type, and the managing subsidiary and parent company were obtained and added during the course of this work.

The catalog is sorted from the gas flares detected the earliest to the latest (based on their first appearance in the original VIIRS Nightfire annual catalogs, ID2012 to ID2020 – “ID_old” field) and numerated generally in the eastwards direction. Newly detected gas flares from 2016 onwards were added below the 2012–2015 entries annually with their respective original Nightfire ID from the first year of observation. Unlike the original Nightfire datasets, the catalog in this study is mostly aimed at preserving the continuous flaring history of observation for each gas flare and therefore uses the old ID classification.

S1.2. Gas flare ID

Gas Flare ID (‘ID_old’) column contains unmodified flare ID obtained from the original VIIRS Nightfire annual catalogs from a respective year of their first observation (2012–2015 annual catalog uses the prefix “2012_”) corresponding to the first Nightfire annual dataset nomenclature. The original VIIRS Nightfire ID is stated in the last columns “ID2012” etc.; note, however, that due to manual modifications in 2017–2020 (merge of “duplicated” (one gas flare split into two IDs) or “halo” ID (thermal halo around the largest gas flares, especially with several flaring stacks in close proximity)), the original ID of the “duplicated” flares or flares with “halo” may not correspond to the original Nightfire ID as the largest (in terms of flared volumes) ID (“parent” ID) was used in this catalog instead.

S1.3. Federal district and subject

Federal districts and federal subjects are the first two highest levels of administrative division of Russia, respectively. Federal subject shapefiles were generated from the geographical coordinates extracted from OpenStreetMap [67]. For reference, federal subject name Cyrillic to Latin transliteration is based on the Wikipedia list (available online at https://en.wikipedia.org/wiki/Template:Subdivisions_of_Russia). Federal districts were assigned based on federal subjects comprising them.

In several cases, federal subjects’ borders from [67] were manually edited as the resulting shapefiles were not accurate enough (e.g., Khanty-Mansi – Yamal-Nenets Autonomous Okrugs’ boundary). In the cases where a single field overlaps with the border between the two regions with gas flares observed in both parts, federal subject was assigned based on the geographical location of the flare (i.e., one field can be located in two federal subjects in the catalog, and flaring volumes are accounted for two regions based on the actual gas flare location). Offshore gas flares were instead assigned the name of the sea they are legally attributed to based on Rosgeofond (Russian Federal Geological Fund) data [37] and compiled subsequently into an artificial “federal district” Shelf of the RF (Russian Federation) as offshore platforms are legally a separated entity.

S1.4. Field or object Name

VIIRS Nightfire gas flare geolocation data was manually intersected with the field and field lease (or subsoil licensing) information acquired from the Map of mineral deposits and Map of subsoil licensing of Russia by Research and Analytical Center “Mineral” [39] as, to our knowledge, it is the only up-to-date (data updated for 01 March 2021 at the time of writing) open source of such information containing oil and gas field boundaries of Russia which is not distributed in the form of a shapefile.

The Map of mineral deposits contains the names of most fields with observed gas flaring. In the case of gas flares from the exploration drillings which had not been mapped yet, the name of the field was left unde-

field, followed by the subsoil lease sector name according to the Map of subsoil licensing (e.g., “? (%Example lease sector name% sector)”), unless such information could be found in oil and gas related mass media based on the license ID. Such fields were re-visited annually for updated information on the field name. Currently, 19 gas fields have their respective field unnamed.

Field names were automatically transliterated from Cyrillic to Latin script. Transliteration of the field names may differ between sources (e.g., “y” and “i”, “ye” and “e”, “yo” and “e”, etc. may be used interchangeably). Note that prefixes meaning cardinal directions were not translated, along with some other prefixes¹. In the case of several large fields subdivided between several companies (e.g., Priobskoye), the block is specified in the field name (e.g., “Srednebotuobinskoye: Central block”).

Most downstream facility names were obtained from the major oil and gas companies annual reports in English. Midstream and downstream object names were obtained from the EnergyBase database [41] (based on the Ministry of Energy of Russia data), or the Wikimapia and OpenStreetMap collaborative mapping projects or official Public cadastral map of Russia by Rosreestr (The Federal Service for State Registration, Cadastre and Cartography of Russia) [42,68,69].

S1.5. Subsidiary and parent company

“Mineral” maps are based on the database from Rosgeolfond, subsidiary of Rosnedra (Russian Federal Agency for Mineral Resources). Rosgeolfond database [37,38] contains the information on the subsidiary in possession of the subsoil license and therefore the field.

Major oil and gas companies, as well as several minor companies, publish lists of their subsidiaries online or in their annual reports. Otherwise the parent company may be mentioned in oil and gas related mass media sources or open data versions of Interfax SPARK system of business credit information.

In several cases, subsidiary companies might have been acquired by the other company or reorganized. Such transitions are shown with “→” symbol with the year of transition mentioned as “(since 20xx)” afterwards. Among the major changes, Rosneft acquired TNK-BP assets in 2013 and Bashneft in 2016 (these dates are not stated in the catalog).

In the case of joint ventures, the share of each shareholder is presented in the ‘Parent Company’ cell, as well as in the list 2 (“List of Joint Ventures”) of the catalog spreadsheet. Legally, several projects (Sakhalin shelf projects (“Sakhalin-1” and “Sakhalin-2”) and Kharyaga field in the Komi Republic) are considered production sharing agreement; this is ignored in the catalog. Note that for the flaring volumes calculations (i.e., parent company annual flaring volumes), flaring volumes are distributed between the companies based on their respective share in the joint venture (not based on the field operator or the company with the largest share) which may differ with the reported data and other sources.

The information on joint venture shares was acquired from oil and gas companies’ web sites, annual reports, oil and gas related mass media or based on the information presented by the World Bank (which was later used to verify the list against later). List of shareholders and their respective shares is refreshed for 2020.

S1.6. Field or object type and predominant (extracted) component

As described in Section 1.1 of the main paper, major extracted component is an important factor in calculating gas flaring environmental emission fees as it is only applicable for associated petroleum gas, or APG, treated as such only when extracted via the oil wells (meaning that natural gas and gas condensate upstream facilities are exempt from increased taxation).

Rosgeolfond database contains information on the field type based on the subsoil license agreement [38]. The open version of the database does not provide the exact levels of oil and gas production, however. Approximately half of the entries in the catalog are classified as single component fields in Rosgeolfond database (predominantly “Oil”, i.e. only oil exploration via oil wells is allowed in the license agreement which automatically assigns ‘APG’ status to the extracted and flared gas) while the other half mostly consists of the ‘Oil&Gas&Condensate’ category. Major oil and gas companies usually present the level of production on their websites or in the annual reports, and the ‘Major Component’ is set accordingly in the catalog. (Note that gas condensate is not distinguished from natural gas in the catalog as their production usually coincides.)

¹ Cardinal directions may be translated in other sources: “north” = “severo-”, “east” = “vostochno-”, “south” = “yuzhno-”, “west” = “zapadno-”. Others: “upper” = “verkhne”, “middle” = “sredne”, “lower” = “nizhne”.

If such information was missing, it was looked for in oil and gas related mass media, scientific papers related to the fields in question, or from VSEGEI (Russian Geological Research Institute) atlas [70] and later checked against the World Bank data. In the worst case, fields without any information had their 'Major Component' left blank ('?' symbol was used) which is applicable for 10 entries.

Several gas fields have facilities dedicated to oil treatment that are specified in Public cadastral map of Russia or Wikimapia (e.g., large Komsomolskoye natural gas field, operated by Gazprom, has an oil processing unit owned by Rosneft) [42,69]. Gas flares attributed to the facilities such as oil treatment unit in the example above have their 'Major Component' set to 'Oil' and their name set to '%Field name% (Oil)' in the catalog, while the rest gas flares of the field have the 'Major Component' set to 'Gas'.

Most downstream facilities are classified as (oil) refineries, gas processing plants (GPP), and liquefied natural gas plants (LNG) in EnergyBase database or in the annual reports of the major companies [41]. (Note that original Nightfire catalog does not separate refineries and gas processing plants.) Petrochemical plants are either defined as such by the companies or can be distinguished based on their production (e.g., polymer products). Midstream category is eclectic as it contains pipeline infrastructure (mostly central control units of the pipeline systems), underground natural gas storage facilities, oil depots, or oil loading racks and terminals. Such objects names were obtained from Public cadastral map of Russia or Wikimapia [42,69].

S1.7. Geographical coordinates, temperature, detection frequency (Pct), and flaring volumes (V, MCM)

Original VIIRS Nightfire geolocation data uses WGS 84 coordinate system of the gas flare contour centroid (see Section 2.1 of the main paper). In the catalog, original centroid geographical coordinates were preserved for the gas flare ID based on the first year of its observation (e.g., if the flare has been observed annually since 2016, catalog will contain the gas flare centroid coordinates from 2016 which would not be updated in the subsequent years). Gas flare coordinates were not corrected for the precise gas flare location (observed in e.g. Google Earth) as high spatial resolution imagery is not available for every gas flare in Russia, and often one Nightfire entry may correspond to a flaring facility consisting of several flaring stacks; another reason is to preserve compatibility with the original annual VIIRS Nightfire datasets.

Minimum, maximum and mean temperatures (in K) were obtained from the original Nightfire on the annual basis. Note that:

- Annual Nightfire temperature data for some flares in 2018–2020 is built up (and will appear identical);
- As “duplicated” gas flares were manually merged in 2017–2020, the temperature data only from the flare ID which the duplicated flares were merged into is presented.

Detection frequency ('Pct') accounts for the relative numbers of flare observation in cloud-free condition (see Equation (3) of the main paper) and is given on annual basis. For “duplicate” detections merged in the catalog, the field is left with “?” in 2017–2019; in 2020, the detection frequency of the “parent” flare ID the other flare data are merged into is stated instead.

In contrast to the original VIIRS Nightfire dataset, flared volumes ('MCM') in the catalog were converted from billion into million cubic meters (BCM → MCM). The reasoning for the transition is a more detailed, site-specific level of this study. In this catalog, “duplicate” detections that were merged had their flared flaring volumes summed up and applied to the “parent” flare ID. Flaring volumes in these columns do not account for the respective share in joint ventures.

S2. Additional figures and tables

Section 2. Method

Figure S1 presents the method flowchart of VIIRS Nightfire algorithm.

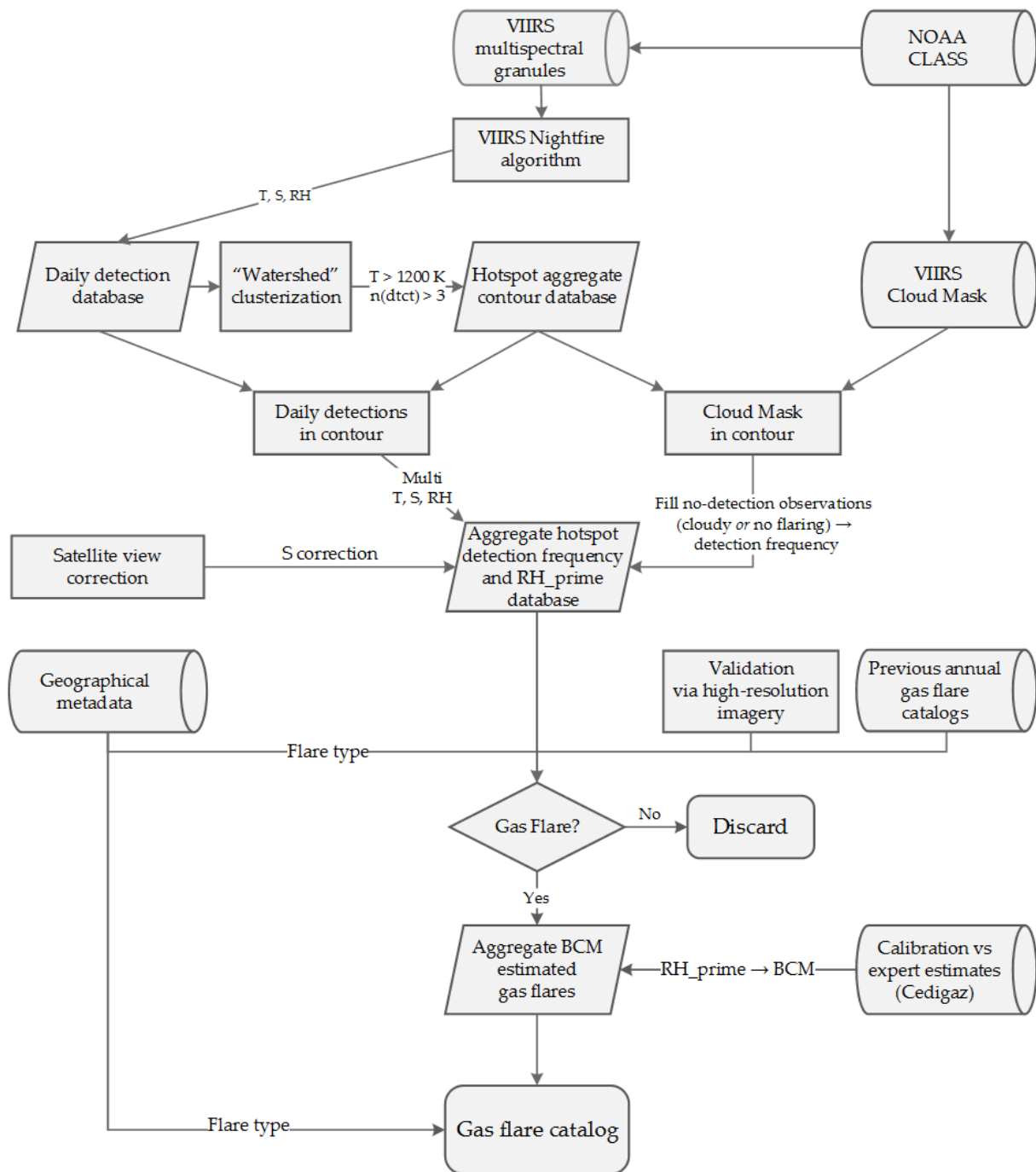


Figure S1. Flowchart of the VIIRS Nightfire gas flare catalog acquisition method.

Section 2.5. Calibration of the flared gas volume estimates based on the average radiative heat of flares

Table S1 specifies exact slope b_1 coefficient and R^2 for the regression with the Cedigaz data presented in Figure 3 in the main paper.

Table S1. Regression through the origin slope coefficient b_1 and R^2 for separate annual VIIRS Nightfire RH' calculations vs. Cedigaz reported datasets in 2012–2019.

Year	2012	2013	2014	2015	2016	2017	2018	2019
b_1	0.0301	0.0297	0.03	0.0285	0.0269	0.0282	0.027	0.0255
R^2	0.847	0.86	0.868	0.814	0.8951	0.833	0.925	0.914

From Table S1 a general trend of decreasing correlation coefficient slope b_1 emerges which leads to an overall better fit of the data ($R^2 = 0.85 \rightarrow 0.9$). To the present day, VIIRS Nightfire uses a correlation coefficient $b_1 = 0.0294$ obtained in a fit with 2012–2017 Cedigaz data (note that for Russia, un-updated gas upstream flaring was applied instead). As since January, 2018 data from M11 SWIR band has been added to the annual VIIRS Nightfire data (VIIRS Nightfire V 2.1 has been updated to VIIRS Nightfire V 3.0), it may be the main explanation for the observed decline in b_1 (i.e., the weight of 1 RH' , MW has increased) as the sensitivity of Nightfire to lesser flares has increased [24]. Another source of possible contribution might be initial underestimation of the flaring volumes (example in Russia is presented in Section 4.2 of the main paper), as well as change in flaring trends of the USA and other major oil producers which, depending on the prevailing scale of gas flares (i.e., their respective gas flaring volumes) in such countries, may increase or decrease Nightfire overall sensitivity causing bias in the estimates as at a typical 1700–1800 K gas flare temperatures, VIIRS Nightfire will be typically able to detect flaring events scaling to burning of c. 20000 m³ / day (7–8 annual MCM) [24,25].

Section 3. Results

Figure S2 presents a screenshot of an example entry from VIIRS Nightfire gas flare catalog in Russia.



Figure S2. An example of gas flare catalog entry in Google Earth.

Section 3.1. Context of the major oil producing and gas flaring countries

Figure S3 demonstrates a comparison of detection frequency versus gas flaring volume scattergrams plotted for Russia and USA.

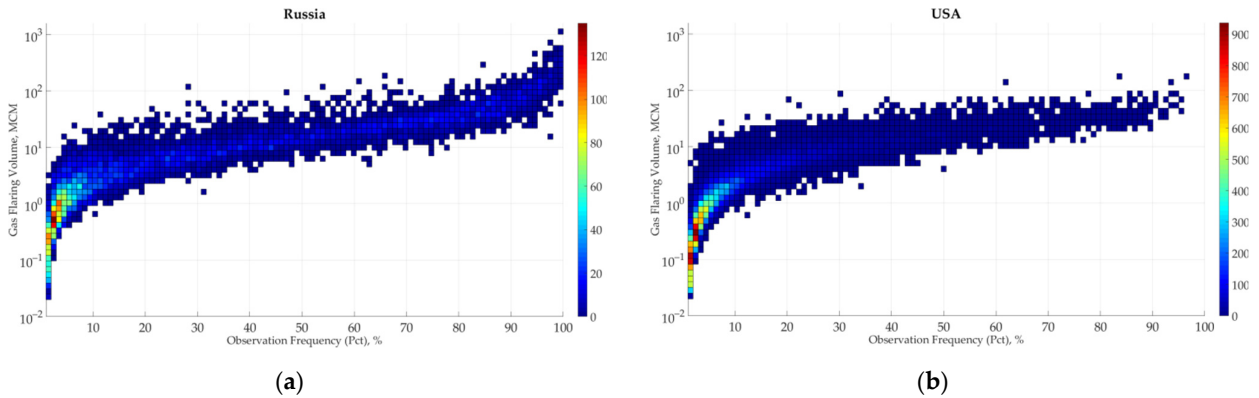


Figure S3. Scattergram VIIRS Nightfire 2012–2020 upstream sector observation frequency *vs.* estimated gas flaring volume (in million cubic meters, log MCM) in (a) Russia and (b) USA.

It is apparent that detected gas flares form a continuous sequence with gas flares in the USA tending to flare less volume per relative detection frequency. It is also evident that the largest flares in Russia fall outside the general distribution presumably because of low or non-existent APG (associated petroleum gas) utilization facilities for some remote oil fields against the background with the dominance of the flares with relatively high APG utilization rates in country. In Russia, a sizable group of infrequent c. 10 MCM flares can be observed which could be attributed to the gas flares in operation –or detectable with VIIRS Nightfire– only during the certain period of the year (high MCM, low detection frequency).

Section 3.2.1. Regional estimates

In Table S2, Nightfire-estimated flaring volumes for the largest flaring fields of Russia are presented.

Table S2. VIIRS Nightfire field-specific flaring volume estimates for high flaring oilfields in Russia(in MCM).

Field	Region	Company	2012	2013	2014	2015	2016	2017	2018	2019	2020
Orenburg: Eastern block	Orenburg	Gazprom Neft	110	129	154	227	196	108	181	99	62
Koshinskoye	Orenburg	SAFMAR	0	0	0	11	16	60	212	474	799
Priobskoye (North)	KhMAO	Rosneft	581	360	205	239	306	219	230	246	106
Yuzhno- Priobskoye	KhMAO	Gazprom Neft	815	744	579	389	121	159	267	253	282
Prirazlomnoye	KhMAO	Rosneft	308	277	348	393	375	352	446	407	343
Samotlor	KhMAO	Rosneft	323	278	219	292	306	176	138	130	137
Tagrinskoye	KhMAO	Russneft (SAFMAR)	302	348	182	257	405	257	196	190	119
Yarudeyskoye	YaNAO	Novatek / Corp. Energy	3	1	22	158	786	741	787	503	369
Novoportovskoye	YaNAO	Gazprom Neft	6	72	56	77	436	933	654	469	476
Vostochno- Messoyakha	YaNAO	Rosneft / Gaz- prom Neft	24	26	40	8	104	230	438	852	763
Vankor	Krasnoyarsk	Rosneft / ONGC / ...	1627	1571	1155	365	292	108	87	84	71
Suzunskoye	Krasnoyarsk	Rosneft	2	1	0	35	196	246	275	251	336
Tagulskoye	Krasnoyarsk	Rosneft	0	1	0	0	6	16	245	345	297
Yurubcheno- Tokhomskoye	Krasnoyarsk	Rosneft	7	14	27	60	56	145	671	1189	1534
Kuyumbinskoye	Krasnoyarsk	Slavneft	9	10	15	18	23	92	220	468	658
Dulisminskoye	Irkutsk	Dulisma	519	661	762	1046	862	1087	1106	1134	1315
Yaraktinskoye	Irkutsk	INK	450	483	541	800	901	1190	694	1088	1074
Ichedinskoye	Irkutsk	INK / JASSOC	0	3	41	106	265	498	506	547	504
Verkhnechonsk	Irkutsk	Rosneft / Beijing Gas	461	451	498	565	588	668	293	152	171
Srednebotuobin- skoye: Central	Yakutia	Rosneft / Indian Oil / BP	5	91	319	301	202	150	404	758	791

Section 3.2.2. *Company level estimates*

Table S3 specifies exact data used for Figure 7 from the main paper.

Table S3. Mean reported liquid hydrocarbon (LH) production, APG production and flaring (as in [1,2]), and Nightfire estimated gas flaring volumes for major producing companies in Russia in 2018–2020.

Company	LH production, mln tons	APG extraction, BCM	Reported flaring, BCM	Nightfire est. flaring, BCM¹
Rosneft	190	31.5	6.4	7.8
Lukoil	79	11.5	0.3	1.7
Surgutneftegas	59	9.5	0.04	0.08
Gazprom Neft	39	13.5	2.1	2.75
Tatneft	28	0.97	0.04	0.07
Gazprom	18	1.66	0.02	0.09
Bashneft	17	0.59	0.07	0.41
Slavneft	12.5	0.82	0.34	0.84
Novatek	8.3	3.2	0.11	0.37
RussNeft	7	2.1	0.09	0.57

¹ Note that in reported data, some joint ventures accounted for their parent companies in Nightfire data are instead presented as separate entities. Here, in Nightfire data, Bashneft and Slavneft estimates are excluded from their parent companies' data (Rosneft and Gazprom Neft).

Section 3.3. *Comparison with the reported gas flaring and oil extraction data*

Figure S4 and Table S4 present a correlation between VIIRS Nightfire estimates and gas flaring data for Khanty-Mansi Autonomous Okrug (KhMAO) reported by the regional authorities [31,32]. Although the correlation with the low number of available data points is strong, the Nightfire estimates deviate from the reported data by a factor of 2 to 3 with a sizable constant offsetting the regression slope. 2016 flaring volumes also stand out from the scatterplot. We assume it to be caused by an emergency event described in Section 4.1 of the main paper.

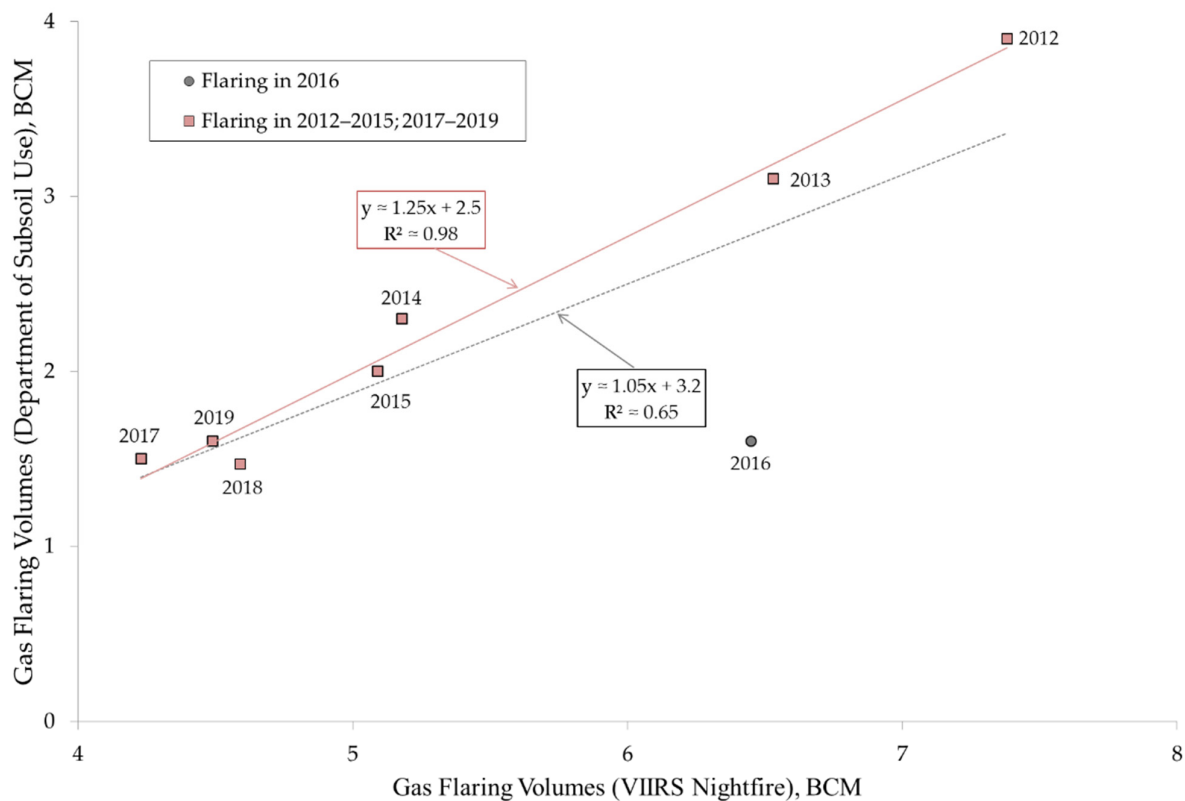


Figure S4. Plot gas flaring volumes (in BCM) in Khanty-Mansi Autonomous Okrug according to VIIRS Nightfire estimates (x axis) vs. regional authorities reported data (y axis) [31,32]. Dotted line is the regression including 2016 data and solid line is the regression with 2016 data excluded. Note that the x axis is offset by 4 BCM.

Table S4. Annual oil and APG production and flaring in Khanty-Mansi Autonomous Okrug.

Source	2012	2013	2014	2015	2016	2017	2018	2019
Oil Prod., mln tons	260	255	250.3	243.1	239.2	235.3	236.5	236.1
APG Prod., BCM	36.2	35.9	33.7	33.9	34.5	35	35	35.8
Reported Flaring, BCM	3.9	3.07	2.3	2.03	1.56	1.5	1.47	1.6
Nightfire Flaring, BCM	7.4	6.55	5.2	5.12	6.5	4.25	4.47	4.55

Section 4.3. Effect of gas composition and combustion efficiency

Figure S5 expands on the estimated gas flare temperature distribution presented for Russia in Figure 11 of the main paper and presents Nightfire estimates for major gas flaring regions of the world. Figure S6 is a scatterplot Nightfire temperature estimates vs. heating value based on reported gas composition for several oil and gas fields in Russia.

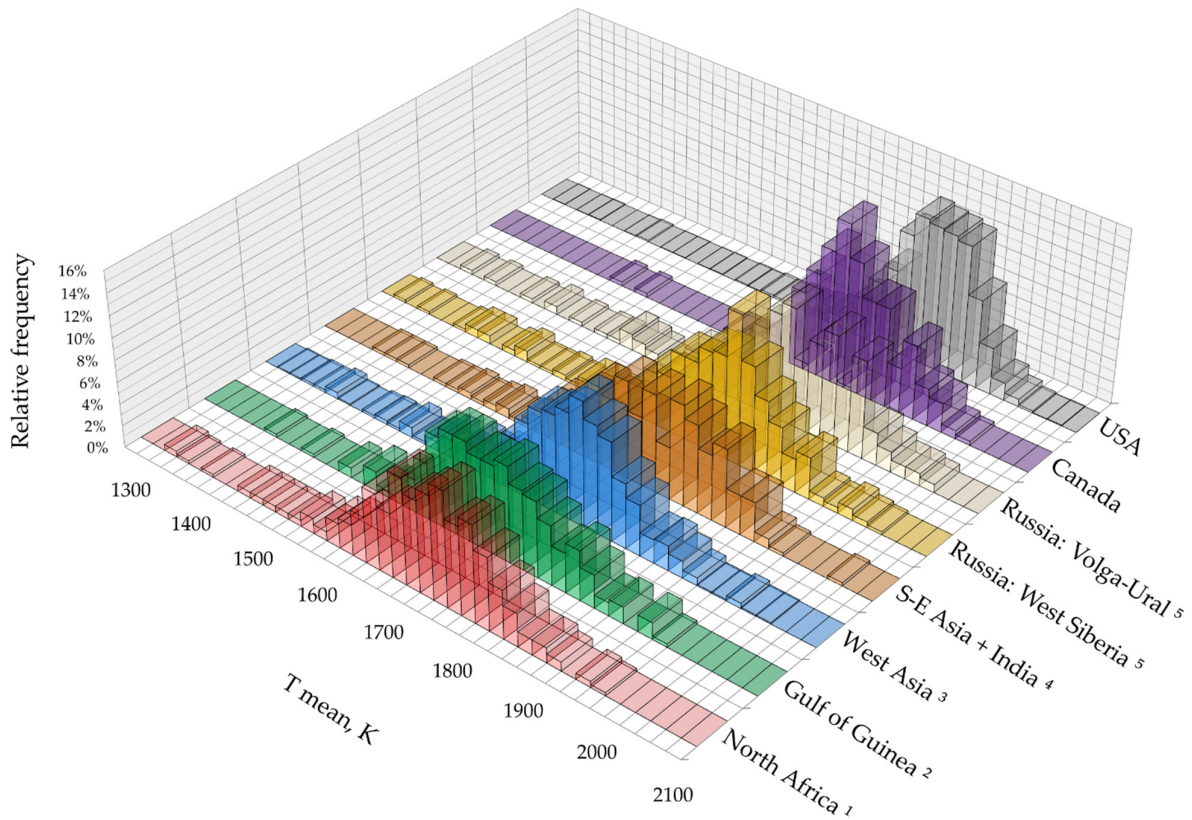


Figure S5. VIIRS Nightfire gas flare mean temperature relative frequency distribution in the regions of the world, 2019.

¹ North Africa includes Libya, Algeria, and Egypt.

² Gulf of Guinea includes Angola, Cameroon, Congo, Côte d'Ivoire, DR Congo, Equatorial Guinea, Ghana, and Nigeria.

³ Western Asia includes Bahrain, Iran, Iraq, Jordan, Kuwait, Oman, Qatar, Saudi Arabia, Syria, and Yemen.

⁴ South-East Asia includes Indonesia, India, East Timor, Myanmar, Malaysia, Philippines, Thailand, and Vietnam.

⁵ For Russia, only oil fields estimates are used.

As seen from Figure S5, gas flaring in Africa experiences the lowest observable temperatures, while the highest observable temperature corresponds to North America. While the latter can be attributed to the prevalence of relatively small gas flares in both Canada and USA which, due to Nightfire detection sensitivity, are usually detected from nadir and, supposedly, during highest efficiency gas burning (e.g., low wind conditions), lower mean temperatures in Africa and West Asia, on the other hand, can either be attributed to moist atmospheric conditions leading to lower signal transmittance (Gulf of Guinea) or lower combustion efficiency and higher tendency for gas flares to smoke. Lower flaring temperatures in North Africa can also be attributed to flaring on natural gas upstream and downstream facilities. If gas and gas condensate field temperature estimates were to be included in Western Siberia data, the mean temperature would have dropped by 50 K, close to Western Asia level.

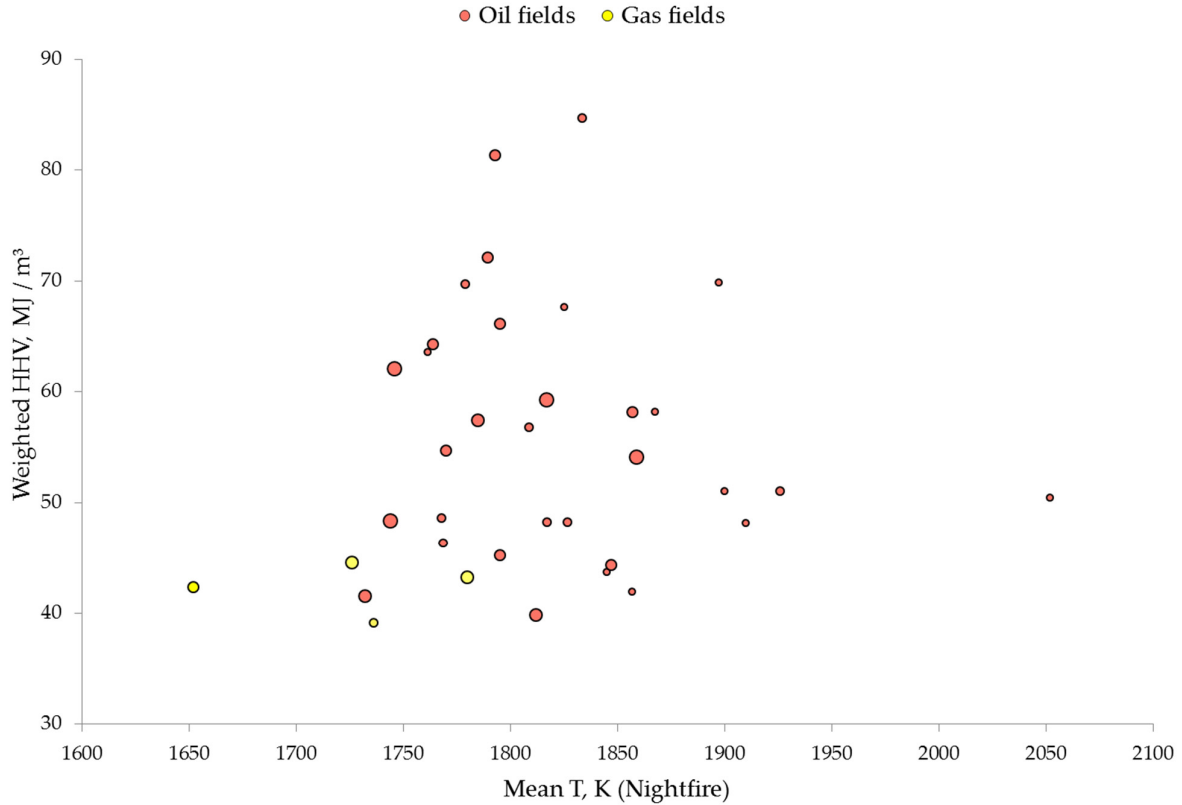


Figure S6. Plot Nightfire mean temperature (in K) *vs.* (volumetric) higher heating value (HHV, in MJ / m³) for fields with APG composition available in literature in Russia, 2012–2015 [71–76]. Size of the marker correlates with estimated gas flaring volume. “Gas fields” correspond to natural gas upstream facilities.

From Figure S6 it is evident that based on APG composition available in literature, there is no significant correlation observed between Nightfire estimated temperature (which is the major contributor to estimates of radiant heat, RH, in MW) and calculated higher heating value of APG. Likewise, estimated flaring volumes (represented by the size of the marker in Figure S6) do not seem to have an impact on correlation. It should be noted, however, that available sources usually present composition of the extracted APG which may change drastically when the residual gas is sent to the flaring stack following the primary processing. Another issue is the temporal and spatial difference (the latter is demonstrated on the example of three different facilities from the Samotlor field [71]) in APG composition which makes most sources outdated for Nightfire observations. It is also possible that ambient factors (such as flare stack construction, prevalent weather conditions which result in different combustion efficiency and, together with satellite view angle, impact the exposure of the flaming body with uneven temperature distribution to the sensor) and processing scheme are more important factors in determining the flaming temperature compared with HHV calculated from the extracted APG composition.